

# Energy & Environmental Science

Volume 16  
Number 1  
January 2023  
Pages 1-324

rsc.li/ees



ISSN 1754-5706

**PAPER**

Jean-Philippe Tessonier *et al.*

An effective strategy to produce highly amenable cellulose and enhance lignin upgrading to aromatic and olefinic hydrocarbons

Cite this: *Energy Environ. Sci.*,  
2023, 16, 97

# An effective strategy to produce highly amenable cellulose and enhance lignin upgrading to aromatic and olefinic hydrocarbons†

Daniel Vincent Sahayaraj,<sup>‡</sup> Lusi A,<sup>‡</sup> Andrew J. Kohler,<sup>ab</sup>  
Hamed Bateni,<sup>ab</sup> Harish Radhakrishnan,<sup>c</sup> Alireza Saraeian,<sup>ab</sup>  
Brent H. Shanks,<sup>ab</sup> Xianglan Bai<sup>c</sup> and Jean-Philippe Tessonier<sup>ab\*</sup>

Lignin is a promising renewable feedstock for the production of valuable phenolic and hydrocarbon building blocks. However, the economic viability of lignin upgrading strategies has so far been hampered by the recondensation of primary products and the preferential formation of char over bio-oil. Here, we demonstrate that lignin pretreatments effectively lower char formation and enhance carbon volatilization during pyrolysis. Various solvolytic and catalytic pretreatments were investigated using sub- and supercritical ethanol and supported metal catalysts. By combining GPC, GC-FID/MS, elemental analysis, HSQC NMR, and TGA, we decoupled the effects of solvolytic and catalytic steps and identified their independent roles on chemical modifications relative to the parent lignin. The pretreatment step enhanced the production of volatiles and concurrently reduced char formation during fast pyrolysis, from 58 C% to 9 C% for lignin deconstructed at 250 °C using Pd/C. The strategy was then extended directly to lignocellulosic biomass (corn stover, switchgrass, red oak) to fractionate and pretreat lignin in a one-pot approach. The lignin oil obtained from this process exhibited an excellent potential to be converted into platform chemicals. Upon catalytic fast pyrolysis of the lignin oil, 11–14 C% aromatic hydrocarbons were produced, while hydrodeoxygenation yielded 34–40 C% of aromatic hydrocarbons (50–56 C% total hydrocarbons). Similarly, the recovered carbohydrates-rich water-soluble fraction was subjected to hydrodeoxygenation and yielded 10–15 C% of aromatic hydrocarbons and 15–29 C% of C<sub>2</sub>–C<sub>6</sub> alkenes (32–74 C% total hydrocarbons). Furthermore, the residual pulp recovered from this method was enriched in sugars and was three times more amenable to enzymatic hydrolysis than the parent biomass. This approach provides new opportunities for the selective and effective conversion of lignin into value-added chemicals and, thereby, enhanced carbon recovery, which is vital for implementing biomass as a feedstock for chemical manufacturing.

Received 18th July 2022,  
Accepted 24th October 2022

DOI: 10.1039/d2ee02304k

rsc.li/ees

## Broader context

To achieve economic viability and thrive, the bioeconomy needs to build on the existing bioethanol infrastructure and broaden the portfolio of products manufactured from biomass. To this end, substantial work has been done to convert cellulose to biobased chemicals through innovations in biocatalysis and thermocatalysis. In contrast, lignin, an aromatic polymer that accounts for 10–25% of lignocellulosic biomass, remains underutilized as a feedstock although its deconstruction could readily supply the chemical industry with platform aromatic hydrocarbons. The challenge comes for lignin's building blocks propensity to repolymerize and form a more condensed network. Reductive catalytic fractionation (RCF), a strategy that combines solvents and metal catalysts to deconstruct lignin and stabilize its building blocks, was recently proposed to directly convert the lignin component in whole biomass. Technologic and economic analyses have highlighted the promise of this strategy but also its present limitations. In particular, new valorization strategies must be explored and developed to also upgrade dimers and oligomers that account for up to 50% of the deconstructed lignin. This work identifies conversion pathways to enhance lignin deconstruction, mitigate carbon loss due to char formation, and facilitate the complete upgrading of lignin to valuable aromatic and olefinic hydrocarbons. When applied to whole biomass, the proposed process also enhances the enzymatic digestibility of cellulose, hence its potential for biofuel and biochemical production. Results obtained for the upgrading of corn stover, an abundant (>75 million tons per year) and underutilized byproduct of corn production, showed a 65% increase in lignin-derived aromatics along with a 200% increase in cellulose digestibility.

<sup>a</sup> Department of Chemical and Biological Engineering, Iowa State University, Ames, Iowa 50011, USA. E-mail: tesso@iastate.edu<sup>b</sup> Center for Biorenewable Chemicals (CBiRC), Ames, Iowa 50011, USA<sup>c</sup> Department of Mechanical Engineering, Iowa State University, Ames, Iowa 50011, USA† Electronic supplementary information (ESI) available: Detailed experimental section; GPC, TGA, HSQC NMR and proximate analysis of the pretreated lignin samples; composition analysis and component balance for the one-pot fractionation and pretreatment of whole biomass; additional HDO results; pictures of the reactor setup used for FP, CFP, and HDO tests. See DOI: <https://doi.org/10.1039/d2ee02304k>

‡ These authors contributed equally to this work.



# 1. Introduction

Lignocellulose comprises about 10–25% lignin, 20–30% hemicellulose, and 40–50% cellulose.<sup>1</sup> Considering its structure, lignin is the largest renewable source of aromatic building blocks in nature and has significant potential to serve as a feedstock for the production of bulk phenolics and aromatic hydrocarbons such as benzene, toluene, and xylene (BTX) that are currently derived from petroleum.<sup>2</sup> However, lignin valorization has proven to be challenging owing to its complex nature and recalcitrant structure, which is why nearly 95% of the extracted lignin is burnt for its energy value instead of being upgraded.<sup>3</sup> When used only as an energy source, lignin is worth only about \$150 per ton; in contrast, its full conversion to aromatics would increase its value to about \$1200 per ton.<sup>4</sup> Therefore, it is critical to design new conversion strategies that overcome present technical hurdles.

The upgrading of lignocellulosic biomass using thermochemical methods typically starts with its fast pyrolysis.<sup>5–7</sup> In this process, biomass or its components are heated to 450–600 °C, in the absence of oxygen, and using fast heating rates to maximize the production of bio-oil over solid products (biochar). Unfortunately, raw bio-oil presents adverse properties due to its high oxygen content (about 40%), namely poor thermal and chemical stability, corrosivity from high acidity, low heating value, and high viscosity compared to petroleum-derived oils.<sup>6,8,9</sup> Several strategies were proposed to lower the bio-oils' oxygen content, overcome its adverse properties, and improve its compatibility with existing infrastructure in the chemical industry. Most of these strategies focus on the production of aromatic hydrocarbons because of their high energy density and important role in chemical manufacturing. Catalytic fast pyrolysis (CFP) is a thermal upgrading strategy that enables the production of BTX, polycyclic aromatic hydrocarbons, alkanes, and olefins.<sup>5,10,11</sup> The best results were obtained with ZSM-5 zeolite due to the unique size and shape selectivity provided by the crystallographic structure of this solid acid catalyst.<sup>12–14</sup> Hydrodeoxygenation (HDO) presents another avenue for upgrading bio-oil by adding hydrogen gas as a reactant. Recently, low-pressure HDO reactions over transition metal oxides, particularly MoO<sub>3</sub>, were shown to completely remove oxygen from biomass/lignin pyrolytic vapors and produce valuable aliphatic and aromatic hydrocarbons.<sup>15,16</sup>

Although studies have shown that it is possible to convert lignin bio-oil into hydrocarbons, the yields are much lower than for whole biomass- and cellulose-derived bio-oils. For instance, 14 C% of aromatics were produced through CFP of pinewood while only 6 C% of aromatics were obtained from its lignin fraction using ZSM-5 at 600 °C.<sup>17,18</sup> Similarly, HDO of cellulose using MoO<sub>3</sub> in a tandem microreactor system at 400 °C generated 84 C% of hydrocarbons while only 30–32 C% were obtained with lignin as the starting material.<sup>19,20</sup> Compared to whole biomass and cellulose, pyrolysis of lignin generates a significantly higher amount of char, which halved the bio-oil yields across all reaction temperatures.<sup>21–23</sup> But, interestingly, when the aromatic hydrocarbon yields generated using a ZSM-5

catalyst at 500 °C were normalized on a pyrolysis vapor basis (in the absence of catalyst), the yields were comparable at 16% for all three components of biomass.<sup>24</sup> Thus, the low hydrocarbon yields obtained for lignin CFP are not due to the nature of the species in the vapor phase but to the efficiency of the volatilization process during the initial pyrolysis step. Therefore, lignin pretreatments that would enhance the volatilization step are vital to increase the production of valuable products and lower carbon losses through char formation.

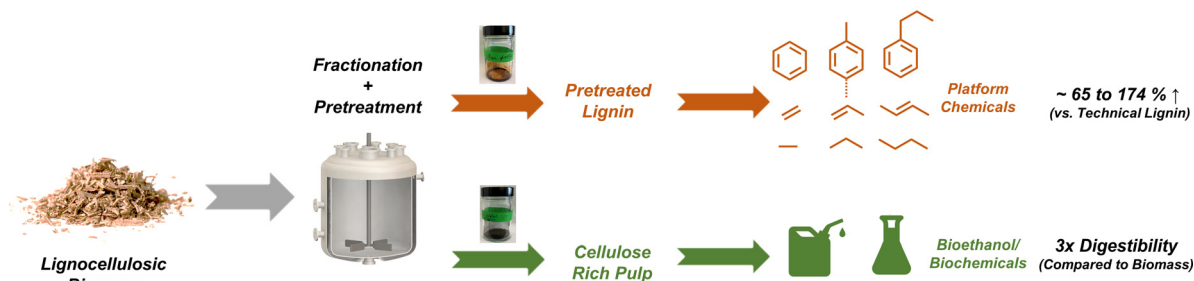
Several research groups have explored pretreatment strategies that could improve the carbon efficiency during catalytic deoxygenation. Feng *et al.* investigated a microwave-assisted formic acid pretreatment as a possible way to improve the production of aromatics for the CFP of lignocellulosic biomass. The pretreated beech wood produced a higher yield of valuable aromatic products than the untreated control (29.8 C% *vs.* 23.2 C%) along with a 10% reduction in char formation.<sup>25</sup> The effects of HCl, NaOH, and H<sub>2</sub>O<sub>2</sub> were also investigated for the pretreatment of kraft lignin prior to its pyrolysis, and upgrading at 650 °C.<sup>26</sup> HCl was found to depolymerize the lignin matrix effectively, increasing the liquid yield, and, at optimized conditions, the selectivity to phenols reached greater than 50% using a large pore zeolite catalyst.<sup>26</sup> More recently, Saracian *et al.* demonstrated that partial depolymerization of lignin using a copper-doped porous metal oxide catalyst in methanol at 300 °C prior to pyrolysis significantly improved the yield of volatile products and decreased the yield of pyrolytic char.<sup>19</sup> Furthermore, the yield of aromatics obtained from HDO using MoO<sub>3</sub> increased by 90% for the depolymerized samples compared to the parent lignin.<sup>19</sup> Although there is a plethora of studies on the pretreatment of biomass/lignin, the exact effect of this additional step remains poorly understood, and the key parameters that would unlock the selective upgrading of lignin to chemicals remain to be identified. Furthermore, accurate carbon tracking to account for losses encountered during the pretreatment step is necessary to draw quantitative conclusions about the beneficial effects of different pretreatments.

Here, we studied the independent and synergistic roles of solvolysis and catalysis during the pretreatment of technical lignin and raw biomass. We focused in particular on their role in enhancing (i) the deconstruction/volatilization of lignin during fast pyrolysis and (ii) the aromatic hydrocarbon yields achieved through subsequent CFP and HDO of the pyrolysis vapors. By combining various complementary characterization techniques, we first gained insights into the chemical transformations occurring during these pretreatments and the parameters that govern the size distribution of the lignin fragments. The product distributions from fast pyrolysis of the parent and pretreated lignin samples were compared to evaluate the effect of the pretreatment on bio-oil vapors and char yields. Next, the pretreated lignin obtained using the optimized reaction condition was upgraded to aromatic hydrocarbons through *ex-situ* CFP and low-pressure HDO, and the obtained yields were compared to the parent lignin.

Using the insights gained from the first part of our study on technical lignin pretreatments, we demonstrate the one-pot







**Scheme 1** Illustration of the whole biomass upgrading strategy described in this study. The lignin oil recovered after one-pot fractionation and pretreatment was successfully upgraded to bulk platform chemicals at higher yields than conventional pulping approaches. The EtOH-insoluble pulp obtained in this study was enriched in sugars and showed improved digestibility, a desired property for bioethanol production.

fractionation and pretreatment of lignin from raw biomass (Scheme 1). The pretreated lignin oil generated through this one-pot approach was readily converted to bio-oil through fast pyrolysis and was funneled to platform chemicals such as aromatics and alkenes at higher yields compared to lignin extracted using conventional fractionation methods. In addition, the residual carbohydrate pulp was preferred for enzymatic hydrolysis and, therefore, should be highly amenable to bioethanol/biochemical production. We further demonstrate the robustness of this ‘one-pot’ approach for various lignocellulosic feedstocks to elucidate the impact of structural variability using compositional analysis and carbon balances. The results provide valuable insights that further advance reductive catalytic fractionation (RCF) and lignin-first fractionation strategies, realizing an ‘ideal lignin stream’ through pretreatment and fractionation that could facilitate complete biomass utilization.

## 2. Results and discussion

### 2.1. Lignin pretreatment

**Independent roles of the solvent and catalyst during pretreatment.** Liquefaction technologies using either water (hydrothermal liquefaction, HTL) or organic solvents (*e.g.*, reductive catalytic fractionation, RCF) effectively deconstruct lignin, affording the highest lignin monomer yields to date.<sup>27–31</sup> While HTL gives excellent results for technical lignin, RCF is superior for whole biomass upgrading as its mild reaction conditions enable a good compromise between delignification and carbohydrate retention,<sup>30,31</sup> and thus better prospects to achieve economic viability for biorefineries.<sup>32</sup> As our ultimate goal for this study was to achieve complete biomass valorization, we started the present work with the RCF of corn stover-derived organosolv lignin in ethanol (EtOH) under subcritical (200 °C) and supercritical (250 °C) conditions for 3 h. Reaction temperature and time were selected based on prior results obtained for the RCF of whole biomass (birch, corn stover) and the solvolysis of technical lignin.<sup>30,33,34</sup> These studies established that fractionation at 200–250 °C for 3 h affords the best tradeoff between the production of lignin monomers and the retention of cellulosic sugars, with ethanol being slightly superior to methanol for lignin solvolysis.

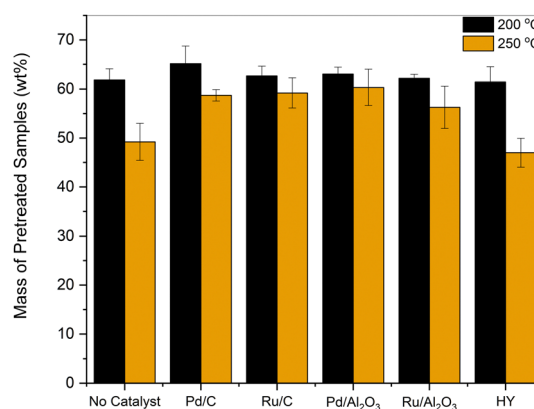


**Fig. 1** Amount of sample (wt%) recovered after treating organosolv lignin in EtOH at 200 and 250 °C for 3 h in the presence of various catalysts.

As shown in Fig. 1, at 200 °C, 61–65 wt% of the pretreated sample relative to the initial lignin was isolated. When the reaction was performed under subcritical conditions, significant differences in product yields were not observed across the tested catalysts. Under supercritical conditions at 250 °C, the yield of the pretreated sample dropped to 50 wt%, and char was observed on the reactor walls in the absence of a catalyst. The benefits of adding a reductive catalyst at 250 °C were evident, as the yield of the products obtained increased by about 10 wt%. In contrast, the addition of HY zeolite, a solid acid catalyst, reduced the product recovery to 46 wt%.

The molecular weight distributions of the pretreated samples were measured to qualitatively assess the extent of deconstruction as a function of reaction conditions. The average molecular weight,  $M_w$ , of the products generated at 200 °C ranged from 1000 to 1386 Da, corresponding to approximately 18–25% of the parent lignin’s molecular weight (Fig. S1a, ESI<sup>†</sup>). An apparent decrease in  $M_w$  to about 520–800 Da with a sharp peak corresponding to monomers around 200 Da was observed for the samples pretreated at 250 °C (Fig. S1b, ESI<sup>†</sup>).

Interestingly, the samples pretreated with and without catalyst showed almost identical molecular weight distributions, meaning the cleavage of the linkages in lignin occurred primarily through solvolysis. However, in the absence of catalyst, a 10 C% loss was observed along with noticeable char deposition on



the reactor walls. These observations, when taken together, indicate that depolymerization and secondary recondensation reactions co-exist and compete with each other. Depolymerization reactions lead to smaller species such as monomers, while repolymerization reactions generate higher molecular weight products, including char, which are not recovered as pretreated lignin oil and are absent in the GPC data.<sup>33,35,36</sup> At higher temperatures, the latter reactions are promoted, and thus the reductive passivation of the reactive intermediates becomes all the more necessary to prevent their repolymerization and enable a higher product recovery.<sup>33,37–39</sup>

**Effect of the pretreatment on elemental composition.** The Van Krevelen diagram in Fig. 2 displays the H/C vs. O/C ratios of the starting lignin and of the pretreated samples. In general, hydrogenation reactions increase the H/C ratio, while the removal of oxygen functionalities decreases the O/C ratio. A greater extent of deoxygenation was observed at 250 °C than at 200 °C, as seen from the lower O/C ratio (0.32 vs. 0.38). In contrast, transition metal catalysts had only little effect on the O/C ratio and predominantly altered the H/C ratio. These results show that deoxygenation is mainly carried out through solvolysis, while the transition metal catalysts are primarily involved in the hydrogenation of the produced fragments.<sup>40</sup>

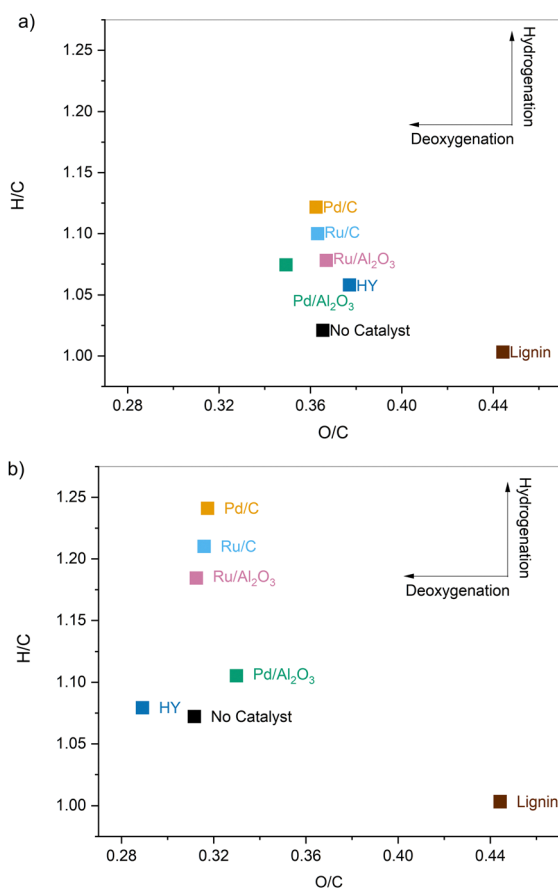


Fig. 2 Van Krevelen diagrams depicting the H/C ratio versus O/C ratio for organosolv lignin and the samples pretreated in EtOH at (a) 200 °C and (b) 250 °C in the presence of various catalysts.

These observations are consistent with recent studies that found that the catalyst was merely responsible for the hydrogenation of the unsaturated sidechains in the solubilized lignin intermediates, while the solvent was primarily involved in the fragmentation of lignin.<sup>41–43</sup> Pd/C had a superior ability to hydrogenate the intermediates compared to other tested catalysts. CO chemisorption revealed that these results cannot be attributed to a difference in the number of active sites for Pd/C compared to other catalysts (Table S1, ESI†). This remarkable catalytic activity was also highlighted in other studies.<sup>44–46</sup>

**Yield and distribution of phenolic monomers.** The volatile monomeric products obtained upon pretreatment of corn stover-derived organosolv lignin as a function of various reaction conditions and catalysts are shown in Fig. 3. Differences were observed for the monomeric yields and product distributions depending on the catalyst used for the pretreatment (Fig. 3). Moreover, higher yields of monomeric product were obtained with supercritical EtOH than with subcritical EtOH (4.2–8.9 C% vs. 1.9–6.1 C%). These results were in line with the molecular weight distributions, where a greater extent of depolymerization was observed after reaction at 250 °C compared to 200 °C. In addition to increasing the rate of lignin depolymerization, supercritical conditions could also enhance the dissolution of lignin, which could potentially contribute to the increase in monomer product yield.<sup>47</sup>

Corn stover lignin is composed of up to ~20% *p*-coumaric acid and ~10% ferulic acid pendant units, which are linked through both ester and ether linkages.<sup>48</sup> These linkages are cleaved under reaction conditions primarily through solvolysis

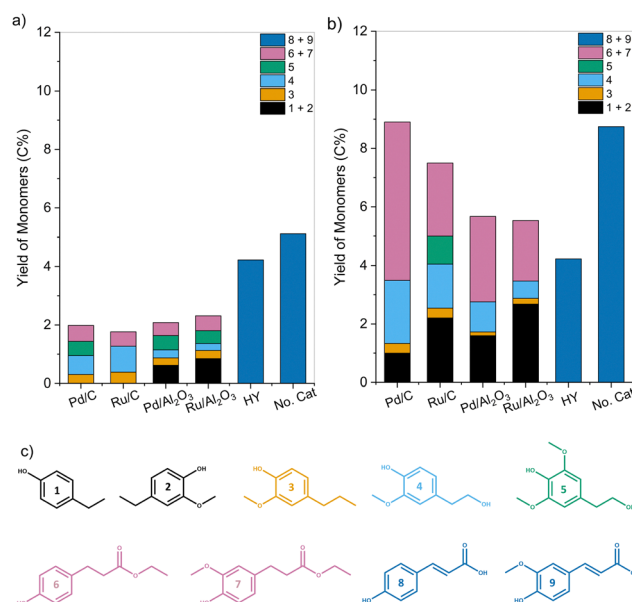


Fig. 3 Yield of phenolic monomers (C%) obtained after subjecting organosolv corn stover lignin to a 3 hour pretreatment in EtOH in the presence of various catalysts at (a) 200 °C and (b) 250 °C. (c) The monomeric products consist of (1) ethyl phenol, (2) ethyl guaiacol, (3) 4-propyl guaiacol, (4) propanol guaiacol, (5) 4-(3-hydroxypropyl)-2,6-dimethoxyphenol, (6) ethyl 3-(4-hydroxyphenyl) propanoate, (7) ethyl 3-(4-hydroxy-3-methoxyphenyl) propanoate, (8) *p*-coumaric acid, (9) ferulic acid.



even in the absence of a catalyst, as evidenced by the yields of monomers **8** and **9**. In the presence of a transition metal catalyst, these hydroxycinnamic acids undergo esterification with EtOH followed by their subsequent hydrogenation to give monomers **6** and **7**.<sup>34,49</sup> Monomers **1** and **2** are formed through decarboxylation followed by hydrogenation of the unsaturated functionalities of formed hydroxycinnamic acids.<sup>50,51</sup> Monomers **3**, **4**, and **5** are formed through the cleavage of  $\beta$ -O-4 linkages in lignin mediated by the supported metal catalyst.<sup>52</sup> Only *p*-coumaric (**8**) and ferulic acid (**9**) were observed for lignin pretreated in the presence of HY zeolite catalyst. Moreover, the yield was lower than for samples deconstructed through solvolysis.

Together, these results indicate that lignin is first solvolytically deconstructed in a polar solvent at elevated temperatures to yield unsaturated products. These products, including monomers, undergo passivation over a hydrogenation catalyst producing saturated alkyl-phenols, guaiacols, ethyl ferulates, and coumarates.

**Heteronuclear single quantum coherence (HSQC NMR) analysis.** Structural information was collected for the parent lignin and the pretreated samples using 2D HSQC NMR (Fig. S2, ESI<sup>†</sup>). For the parent corn stover organosolv lignin, peaks corresponding to  $\beta$ -O-4 linkages were prominent in the side chain region of the NMR spectra. The peak corresponding to  $\gamma$ -*p*-coumaroylated  $\beta$ -ether units ( $\beta$ -O-4 (*p*CA)) was also observed in this region. Hydroxycinnamic acid peaks (*p*CA and FA), which are characteristic of corn stover lignin, were observed in the aromatic region. For a quantitative comparison, the number of interunit linkages from lignin and pretreated samples was estimated through the volume integration of HSQC spectra cross signals (eqn (S1), ESI<sup>†</sup>). The concentration of  $\beta$ -O-4 linkages, defined as the integration ratio of  $\beta$ -O-4 to aromatics ( $S_{2/6}$ ,  $S'_{2/6}$ ,  $G_2$  subunits), was found to be 30% for the parent lignin, which was in agreement with previous studies.<sup>53</sup> Upon pretreatment, the signals of  $A_\alpha$  and  $A_\beta$  corresponding to benzylic alcohols and secondary alkyl protons of  $\beta$ -O-4 linkages decreased due to the scission of C–O–C linkages. The temperature was found to be the main driver for the cleavage of  $\beta$ -O-4 linkages as the  $\beta$ -O-4 concentration dropped to 6% when solvolysis was performed at 250 °C in the absence of any catalyst. Catalyst offered only modest gains, and further lowered the  $\beta$ -O-4 concentration to 2.3% when the pretreatment was performed at 250 °C in the presence of Pd/C.

The increase in the presence of ethyl 3-(4-hydroxyphenyl) propanoate (dihydro *p*CA ethyl ester) and ethyl 3-(4-hydroxy-3-methoxyphenyl) propanoate (dihydro FA ethyl ester) C–H cross signals along with the disappearance of *p*CA and FA signals were observed for samples pretreated using a metal catalyst. These results are consistent with the major lignin monomer products detected by GC-FID/MS. These insights further corroborate that lignin is deconstructed solvolytically, and the heterogeneous metal catalyst is responsible for the stabilization of the extracted monomers through reductive chemistry. The mechanistic insights gained from elemental analysis (Van Krevelen diagrams), GC-FID/MS analysis of the monomers, and HSQC NMR analysis of the pretreated samples are further summarized in Fig. S3 (ESI<sup>†</sup>).

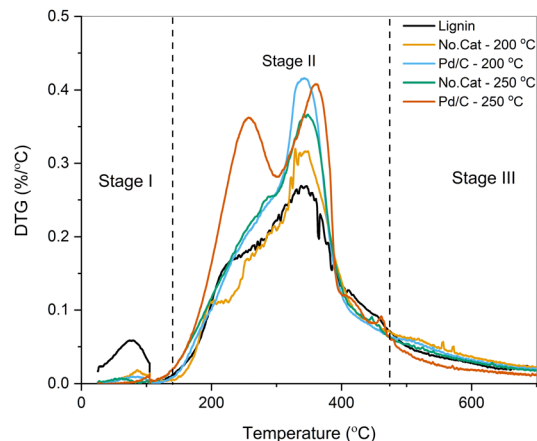


Fig. 4 DTG curves of lignin and representative pretreated samples.

**Thermogravimetric analysis (TGA) of the pretreated samples.** TGA was performed as the rate of volatilization and the associated weight loss is influenced by the inherent structure and the various functional groups present in lignin. The differential thermogravimetric (DTG) profiles obtained from the TGA of the starting lignin and representative pretreated samples are shown in Fig. 4 (TGA in Fig. S4, ESI<sup>†</sup>). The thermal decomposition of lignin during TGA is known to occur in three stages: (i) removal of moisture and light volatiles (50–150 °C), (ii) decomposition/volatilization of lignin to phenolics and other light molecules (150–470 °C), (iii) the final stage (>470 °C) is attributed the decomposition of the more thermally stable groups present in lignin, but with a noticeably lower rate compared to the second stage.<sup>54–56</sup>

As seen from the DTG curves, a larger fraction of the pretreated samples was volatilized compared to the parent lignin. The first contribution at ~250 °C is related to the devolution of small phenolic compounds upon  $\beta$ -ether cleavage, the corresponding release of H<sub>2</sub>O, and the release of light gases from the cleavage of lateral chains in the lignin polymer.<sup>57</sup> This contribution was prominent for pretreated samples, especially for the sample treated using Pd/C at 250 °C, possibly due to the volatilization of monomeric species. The peak at 340–350 °C corresponds to the decomposition of higher molecular weight phenolics, and the rate of volatilization was higher for the pretreated samples due to their partial deconstruction through solvolysis (*vide supra*).<sup>58</sup> Proximate analysis for all the samples is reported in Fig. S5 (ESI<sup>†</sup>). The weight percentage of the volatiles fraction in the parent lignin was 63 wt%, while the pretreated samples showed a notable increase. Higher fractions of volatiles are preferred for lignin upgrading through pyrolysis, CFP, and vapor-phase HDO. By combining solvolytic deconstruction with Pd/C at 250 °C, the volatile content increased to 83 wt% along with a concomitant decrease in fixed, non-volatile, carbon (14 wt% vs. 26 wt%).

## 2.2. Upgrading of pretreated lignin through fast pyrolysis, catalytic fast pyrolysis, and hydrodeoxygenation

**Char yields obtained from fast pyrolysis of pretreated samples.** The fast pyrolysis of the parent lignin and pretreated samples was carried out at a temperature of 500 °C.



The quantified products include GC-FID/MS detectable phenolic monomers and light gases, as well as char (Fig. S6, ESI†). Since the pretreatment enhanced the fraction of volatiles formed during pyrolysis, it conversely reduced the formation of reactive species that could polymerize and form char (Fig. 5).<sup>19,59,60</sup> In general, samples pretreated in supercritical EtOH produced less char than samples pretreated under subcritical conditions due to a greater extent of depolymerization. Pd/C was the most effective catalyst under all conditions, with significant benefits on char formation compared to the solvolytic deconstruction alone (30.7 C% vs. 38.7 C% at 200 °C and 8.8 C% vs. 29 C% at 250 °C).

It has been previously reported that the unsaturated C=C bond located in the phenolics side chains has a strong propensity towards (re)polymerization reactions.<sup>61,62</sup> In a follow-up study, lignin-derived monomers were pyrolyzed to identify the mechanisms leading to char formation.<sup>63</sup> It was observed that the extent of secondary char formation was strongly related to the types of functional groups on aromatic side chains, decreasing in the order of (C=C) > (C=O) > (O-CH<sub>3</sub>).<sup>63</sup> Here, the hydrogenation of unsaturated bonds attenuated the formation of char through secondary reactions. Moreover, the combined yields of CO and CO<sub>2</sub> were lower for the pretreated samples, potentially due to the lower number of C-O bonds susceptible to decarbonylation or decarboxylation reactions. Overall, the

pretreatment step successfully reduced the yield of pyrolytic char from 58.4 C% for lignin to 8.8 C% for the sample deconstructed at 250 °C using Pd/C and enhanced the formation of volatile species.

**Phenolic monomers obtained upon fast pyrolysis.** The identity and yield of phenolic monomeric products generated during fast pyrolysis at 500 °C, as a function of pretreatment temperature and catalysts, are presented in Fig. 6. In most cases, the pretreatment significantly improved the yield of monomeric products generated during fast pyrolysis compared to the parent lignin. The total phenolic monomeric product yield for the parent lignin was 13.72 C%, with 4-vinyl phenol (VP) and 4-vinyl guaiacol (VG) as the primary products (VP + VG = 10.63 C%). These compounds can be generated through the degradation of hydroxycinnamic acids and the cleavage of β-aryl ether linkages in lignin.<sup>64,65</sup> Along with these compounds, 4-ethyl phenol (EP), 4-ethyl guaiacol (EG), phenol, guaiacol, and cresols were also generated. The sample deconstructed using subcritical EtOH showed an increase in monomer yield to 17.00 C% while maintaining high selectivity to VP and VG (12.76 C%). Deconstruction through supercritical EtOH showed an increase in EP and EG with a total monomer yield of 18.20 C%, while the yield of VP + VG increased only slightly (10.99 C%).

In contrast, samples pretreated using transition metal catalysts showed a decrease in VP and VG formation with a concomitant increase in EP and EG yields compared to that of lignin. Additionally, the formation of ethyl 3-(4-hydroxyphenyl) propanoate and ethyl 3-(4-hydroxy-3-methoxyphenyl) propanoate (dihydro *p*CA + FA) ethyl ester) was also observed. For samples depolymerized using Pd/C at 250 °C, the yield of dihydro *p*-coumaric acid ethyl esters increased to 9.8 C%, while the yield of VP + VG dropped to 2.5 C%.

These results corroborate our previous observation that unsaturated functionalities present in lignin were reduced during pretreatment, leading to the formation of ethyl phenolics and dihydro *p*-coumaric acid ethyl esters instead of vinyl phenolics.

**Rationalizing the difference in char yields among various pretreatments.** In an attempt to rationalize the differences observed in the decomposition/volatilization of the pretreated samples for various catalysts and reaction conditions, the reduction in char yields was plotted against the length of the vector between lignin and the pretreated sample in the Van Krevelen diagram (Fig. 7). This distance indicates the relative extent of deoxygenation and hydrogenation compared to the parent lignin. As can be seen in Fig. 7, a strong correlation exists between both measures. In contrast, the decrease in guaiacyl units revealed by the lower S/G ratios for the pretreated samples compared to the parent lignin (eqn (S1) and Fig. S2, ESI†) only had a marginal effect equivalent to a distance of ~0.01 in Fig. 7. Guaiacyl units were previously shown to be a strong contributor to char formation.<sup>63</sup> However, no correlation between char yield and S/G ratio was observed for our set of samples. Overall, catalysts with a higher hydrogenation capacity produce a lignin fraction that generates a higher bio-oil

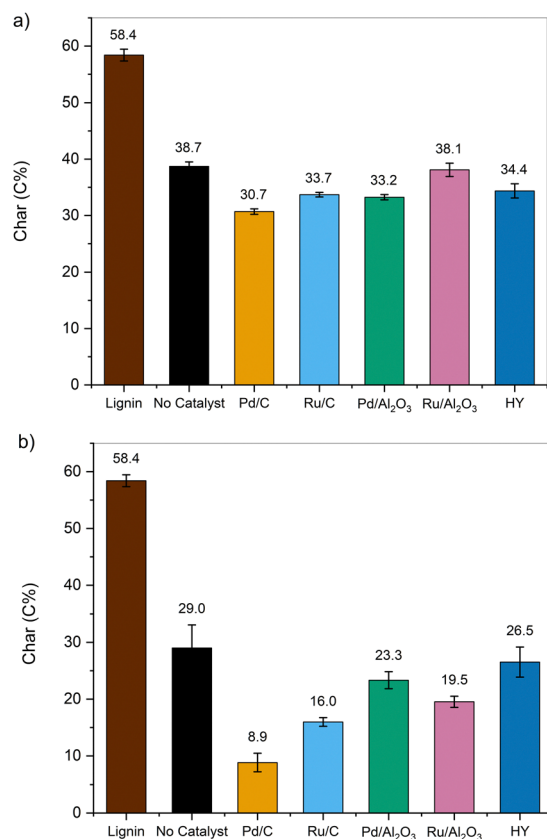


Fig. 5 Char yields (in C%) measured after fast pyrolysis at 500 °C of the parent lignin and lignin samples pretreated in EtOH at (a) 200 °C and (b) 250 °C in the presence of various catalysts.





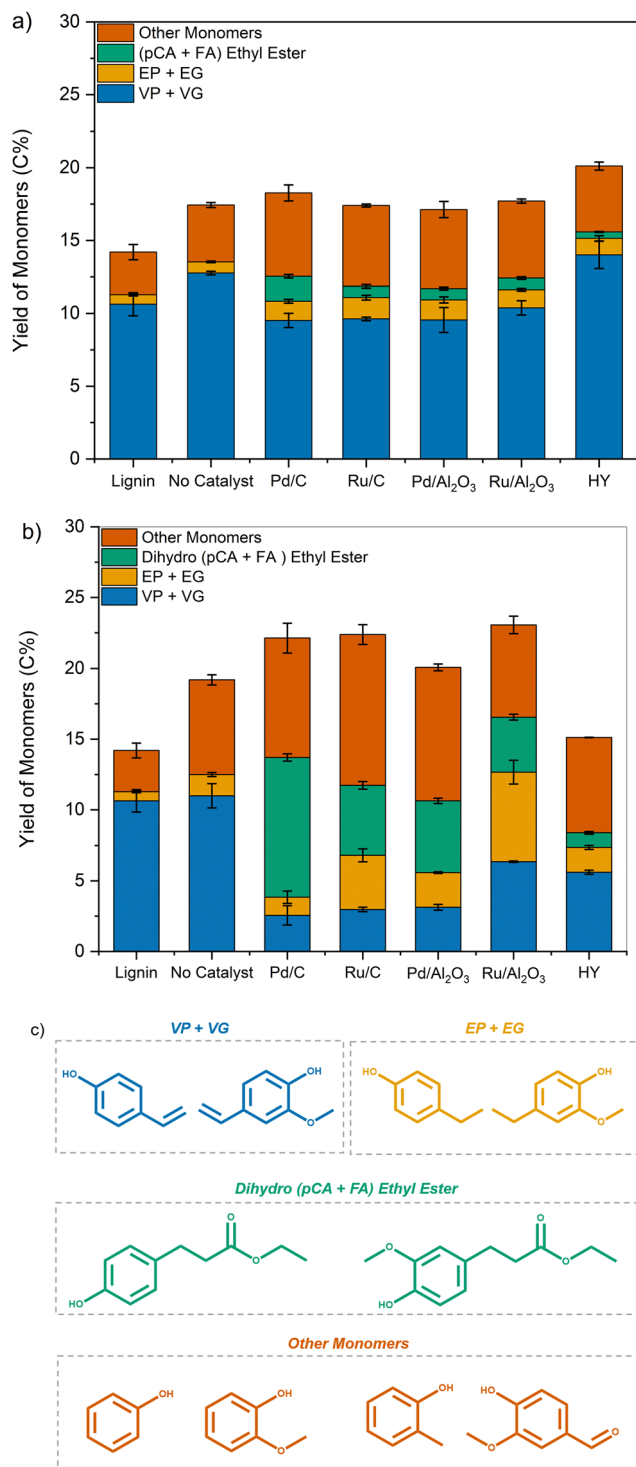


Fig. 6 Yields of phenolic monomers (C%) obtained for the fast pyrolysis at 500 °C of lignin and samples pretreated in EtOH at (a) 200 °C and (b) 250 °C in the presence of various catalysts. (c) Molecular structures of the corresponding monomeric products.

yield during pyrolysis. Furthermore, the depolymerization and the associated deoxygenation of lignin during pretreatment also improve the volatility of the starting material. The molecular weight distribution is one of the essential characteristics

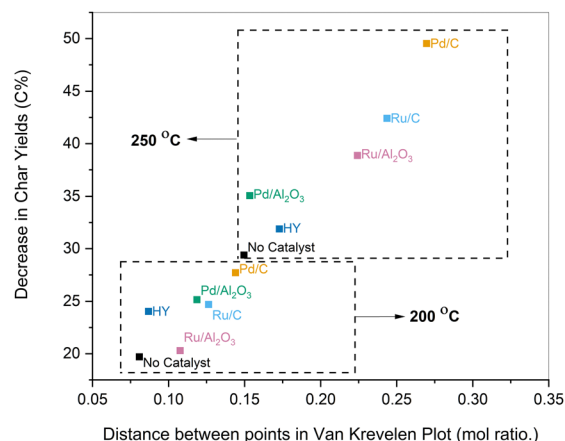


Fig. 7 Reduction in char yields relative to lignin (C%) plotted against the distance between coordinates of lignin and pretreated samples in the Van Krevelen diagram for various catalysts and temperatures.

of lignin, which significantly influences the pyrolysis product distribution. A combination of experimental and modeling insights provided by Marathe *et al.* revealed that heavier molecules tend to polymerize faster than lighter molecules, which results in higher char yields.<sup>66</sup> In essence, the partial depolymerization, deoxygenation, and hydrogenation of the unsaturated functionalities present in lignin attenuate secondary reactions during pyrolysis and subsequently improve bio-oil formation.

**CFP and HDO of samples pretreated using Pd/C at 250 °C.** The sample treated using Pd/C at 250 °C produced the lowest amount of char among all tested pretreatments, leading to a higher fraction of carbon being volatilized. CFP and HDO of the parent lignin and sample pretreated using Pd/C at 250 °C were therefore conducted, and the yields of the products obtained are reported in Fig. 8. For these experiments, the volatiles

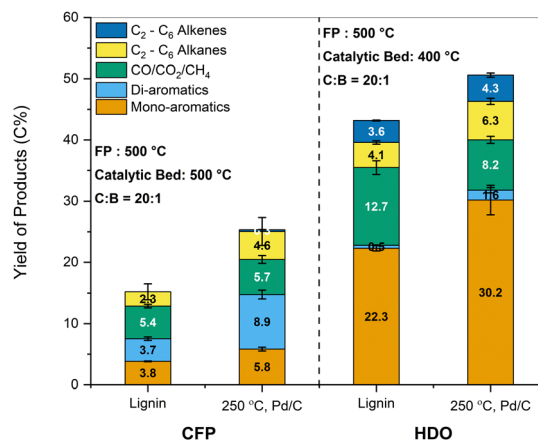


Fig. 8 Carbon yields of products obtained from CFP and HDO of lignin and sample pretreated in EtOH at 250 °C over Pd/C catalyst. Reaction conditions: CFP (ZSM-5 (Si/Al = 15) catalyst, fast pyrolysis temperature (FP): 500 °C, catalytic bed temperature: 500 °C, catalyst : biomass ratio = 20 : 1) and HDO (MoO<sub>3</sub> catalyst, fast pyrolysis temperature (FP): 500 °C, catalytic bed temperature: 500 °C, catalyst : biomass ratio = 20 : 1).





generated upon pyrolysis of the starting material were carried to the catalytic bed for upgrading. It is important to note that the carbon yields reported in Fig. 8 are calculated relative to the carbon present in the pretreated sample used for the CFP and HDO experiments. CFP exclusively produced aromatic hydrocarbons, namely BTX, ethylbenzenes, and naphthalenes. The total yield of aromatics (mono-aromatics and di-aromatics) generated upon lignin CFP was 7.53 C%, which was consistent with prior studies.<sup>58,67</sup> In contrast, the aromatic yield almost doubled to 14.76 C% for the pretreated sample. A 52% increase in mono-aromatics yields such as benzene, toluene, and xylenes was observed. The yield of di-aromatic hydrocarbons also increased from 3.57 C% to 8.55 C% for the pretreated sample.

The same samples were also subjected to HDO for comparison. The combined yields of mono-aromatics increased for the pretreated samples to 30.2 C% compared to 22.3 C% for the parent lignin. The yield of compounds such as benzene and ethylbenzene decreased slightly for the pretreated samples, while the yield of propyl benzene increased substantially from 0.95 C% to 6.10 C%. The change in selectivity could be explained by the presence of propyl guaiacol and propanol guaiacol as monomers in the pretreated sample. Saracian *et al.* reported the formation of propyl benzene as a primary product during the HDO of propyl phenol using MoO<sub>3</sub> at 400 °C.<sup>68</sup> Similarly, Guan *et al.* reported a 98% yield of propyl benzene over Rh/Nb<sub>2</sub>O<sub>5</sub> catalyst under 0.5 MPa H<sub>2</sub> using 4-propyl guaiacol as the starting compound.<sup>69</sup> In contrast to CFP, the formation of di-aromatics such as naphthalenes accounted for less than 2 C%. The yield of alkenes such as ethylene, propylene, and butene improved moderately upon pretreatment. Thus, the beneficial impact of the solvolytic and catalytic pretreatment was also reflected in enhanced aromatic and aliphatic hydrocarbon yields after CFP and HDO.

### 2.3. One-pot fractionation and pretreatment of lignin from whole biomass and upgrading to hydrocarbons

**Mass balance and composition analysis of products recovered after pretreatment.** As the pretreatment showed clear benefits on bio-oil and CFP/HDO product yields for corn stover organosolv lignin, we further investigated if this strategy could be directly applied to whole biomass. This proposed one-pot approach was explored using the most promising pretreatment conditions identified in the first part of the work, namely in EtOH at 250 °C with Pd/C. Supercritical EtOH served as the reaction medium to extract and depolymerize lignin from the lignocellulose matrix, and the Pd/C catalyst enabled the reductive passivation of the intermediates. The overall mass balance and composition of the products are presented in Fig. S7 (ESI<sup>†</sup>). An upper and lower bound estimate for the amount of EtOH-insoluble pulp recovered is also reported to account for the interference of the Pd/C catalyst present in the solid residue during mass measurements. Based on the guidelines established by Abu Omar *et al.* on evaluating the fractionation efficiency, glucan or cellulose, xylan or hemicellulose, and lignin component balance are reported for the three feedstocks in Fig. 9, and Fig. S8 (ESI<sup>†</sup>).<sup>70</sup> Cellulose retention in the EtOH-insoluble pulp increased in the

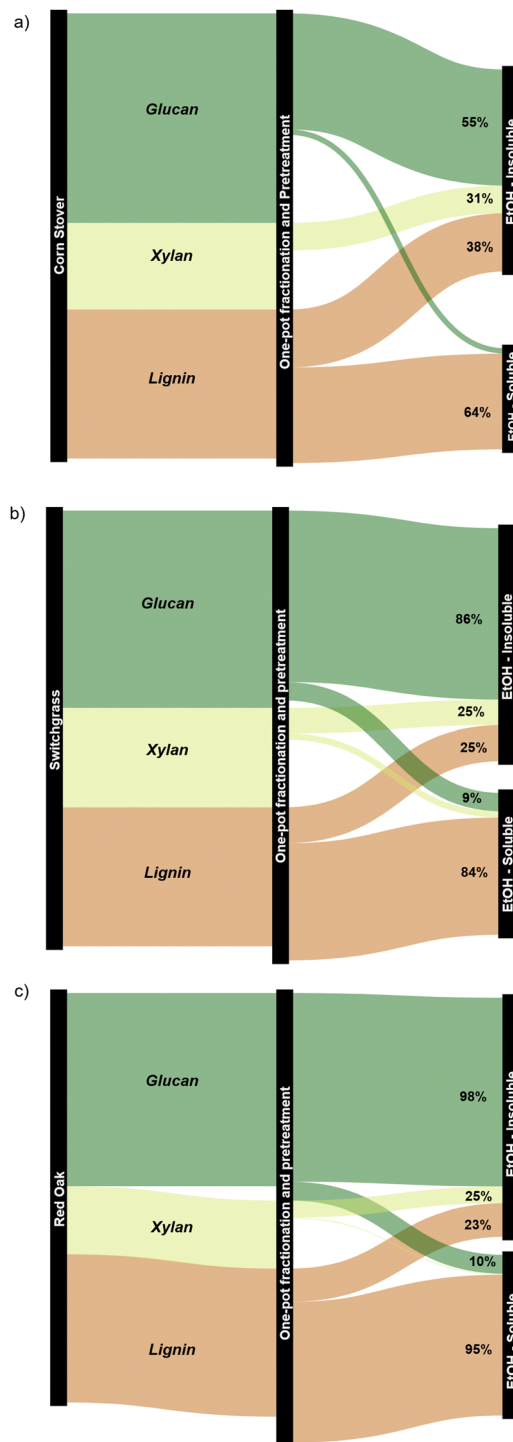


Fig. 9 Component balance (upper bound values) for the products obtained from the one-pot fractionation and pretreatment of whole biomass in EtOH at 250 °C using Pd/C for (a) corn stover, (b) switchgrass, and (c) red oak. The corresponding component balances with the lower bound values are presented in Fig. S8 (ESI<sup>†</sup>).

order of corn stover (55 wt%) < switchgrass (86 wt%) < red oak (98 wt%) for the feedstocks tested. Xylan retention in the EtOH-insoluble pulp varied between 24 and 31 wt% for the feedstocks. Van den Bosch *et al.* reported that the higher retention



of glucan compared to xylan in the pulp is due to better protection of glucose in the crystalline structure, while xylose in the amorphous hemicellulose is more prone to solvolysis.<sup>30</sup> The low mass balance closure for xylan sugar can be attributed to the solvolytic deconstruction of these sugars during the reaction. As described in previous studies, the C<sub>5</sub> and C<sub>6</sub> sugars solubilized in the solvent are recovered as their corresponding ethyl analogs, such as ethyl xylopyranoside and ethyl glucopyranoside. The remaining solubilized C<sub>5</sub> and C<sub>6</sub> sugars are likely to be present as ethylated sugar di- and oligomers and are not accounted for during biomass composition analysis.<sup>31,52,71</sup>

The ethanol-soluble fraction was rich in lignin extracted from the lignocellulose matrix. The extent of extraction varied between 64 and 95 wt% and was heavily dependent on the nature of the biomass sample. In some cases, the lignin component balance was greater than 100%, likely due to the incorporation of EtOH into the depolymerized lignin or the

overestimation of the weights on the EtOH-insoluble pulp caused by the Pd/C catalyst, particularly for the upper bound measurements.

**Characterization of the EtOH-soluble fraction.** The pretreated lignin oil obtained from liquid-liquid extraction of the EtOH-soluble fraction was characterized by GPC, GC-FID/MS, elemental analysis, and fast pyrolysis at 500 °C. The results, along with the organosolv pretreated lignin oil for reference, are presented in Fig. 10. The weight-averaged molecular weights of the oils ranged between 390 and 470 Da, which demonstrated that the lignin fraction from the starting feedstocks was successfully depolymerized into smaller molecules. The total monomeric product yields varied between 11 and 16 wt% relative to the lignin content present in the starting biomass. Notably, the yield of monomers was almost two times higher for pretreated oils obtained directly from biomass compared to organosolv lignin. During organosolv extraction of

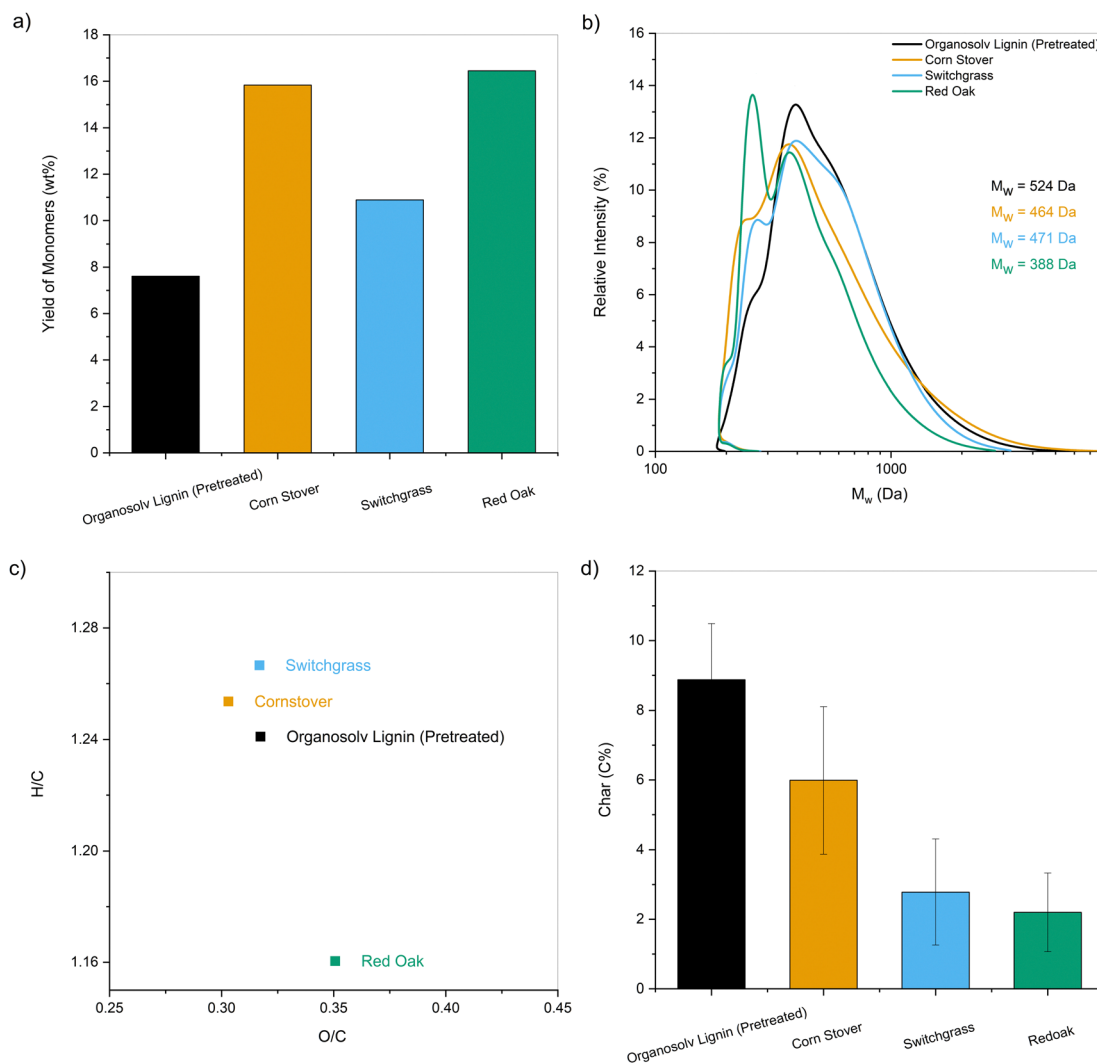


**Fig. 10** Characterization of the pretreated lignin oil obtained from the one-pot fractionation and pretreatment of whole biomass at 250 °C in EtOH over Pd/C. (a) Yield of monomers (wt%) relative to lignin content present in the starting biomass; (b) molecular weight distributions along with their average M<sub>w</sub>; (c) Van Krevelen diagram; (d) char yields (C%) obtained after fast pyrolysis at 500 °C. The results for pretreated organosolv lignin are also provided for comparison.



lignin from biomass, acid-catalyzed cleavage of  $\beta$ -O-4 linkages and ester bonds occurs, leading to a more condensed structure than native lignin.<sup>72</sup> Furthermore, Phongpreecha *et al.* demonstrated that the  $\beta$ -O-4 content present in the starting feedstock is directly proportional to the maximum achievable monomeric product yields.<sup>73</sup> Elemental analysis also revealed that the pretreated lignin oil obtained from biomass was similar to the oil obtained from organosolv lignin, indicating that hydrogenation and deoxygenation reactions occurred during the one-pot fractionation and pretreatment. When the pretreated samples were subjected to fast pyrolysis at 500 °C, the char yields were also remarkably lower (<6 C%) for all the biomass samples tested.

**Upgrading of the recovered lignin fraction through CFP and HDO.** The lignin oil samples obtained from one-pot fractionation and pretreatment were subjected to CFP and HDO to understand if the trend between char and product yields shown in Fig. 8 can be generalized (Fig. S9, ESI<sup>†</sup>). The reported total aromatic (mono- and di-aromatic) product yields during the *ex-situ* CFP of lignin using acidic zeolites are around 7–9 C%.<sup>17,58,74</sup> As shown in Fig. S9a (ESI<sup>†</sup>), the total aromatic product yields upon CFP for lignin oils obtained from one-pot treatment was between 11 and 14 C% depending on the feedstocks tested.

Similarly, alkene and aromatic hydrocarbon yields obtained for HDO of the lignin pyrolytic vapors using MoO<sub>3</sub> catalyst range between 16 C% and 29 C%.<sup>16,19,68,75</sup> As observed for CFP, an increase in yields of hydrocarbons was observed up to 33–36 C% for pretreated lignin oils obtained from biomass (Fig. S9b, ESI<sup>†</sup>). Further HDO optimization was performed by increasing the MoO<sub>3</sub> catalyst to 20 mg for the lignin oils obtained from the one-pot fractionation and pretreatment of biomass. Compared to technical lignins, nearly twice the amount of carbon was volatilized during pyrolysis for the pretreated samples. Thus, the proportional increase in MoO<sub>3</sub> kept the mass ratio of pyrolysis vapors to catalyst loaded constant for all samples. Fig. 11 presents the carbon yields obtained for the HDO of the one-pot pretreated lignin oils along with other technical lignins (the corresponding product distributions are provided in Table S2, ESI<sup>†</sup>). The yield of hydrocarbon-range products was significantly higher for the one-pot fractionated and pretreated samples than for the technical lignins (49–56 C% vs. 20–30 C%). It was apparent that lignin oil obtained after pretreatment could reduce the overall yield of char and increase the amount of volatilized carbon to increase the yield of valuable products upon upgrading.

**Upgrading of the recovered water-soluble fraction through HDO.** In addition to lignin oil, the one-pot fractionation of whole biomass produced a water-soluble fraction rich in sugars. This fraction was recovered, dried, and subjected to HDO using the same reaction conditions as for the upgrading of lignin oil. HDO was preferred over CFP due to the higher hydrocarbon yields achieved in the case of lignin oil and the potential for using a single process to upgrade all EtOH-soluble products, circumventing the need for an extraction/separation step. Fig. 12 shows that in addition to 10–15 C% of mono-aromatics,

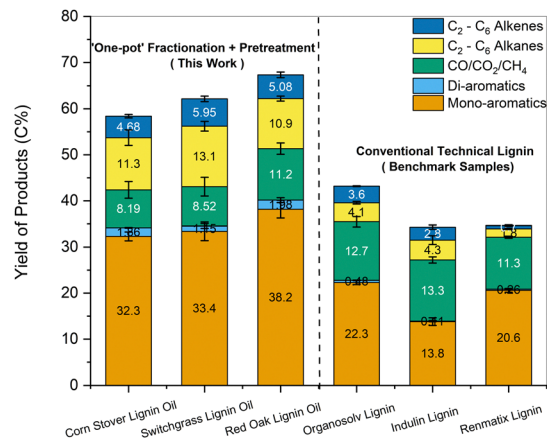


Fig. 11 Carbon yields of products obtained from HDO of the lignin samples after 'one-pot' fractionation and pretreatment of whole biomass. Results obtained with conventional technical lignin samples are also provided for comparison. Conditions: MoO<sub>3</sub> catalyst, fast pyrolysis: 500 °C, catalytic upgrading: 400 °C, catalyst : volatile = 40 : 1.

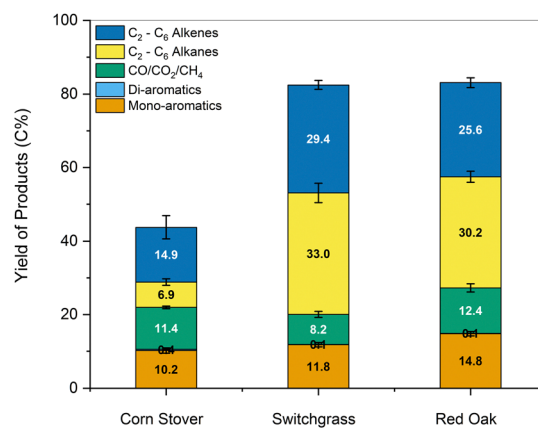


Fig. 12 Carbon yields of products obtained from HDO of the water-soluble fraction recovered after 'one-pot' fractionation and pretreatment of whole biomass. Conditions: MoO<sub>3</sub> catalyst, fast pyrolysis: 500 °C, catalytic upgrading: 400 °C, catalyst : volatile = 40 : 1.

HDO of this fraction produced a significant amount of valuable C<sub>2</sub>-C<sub>6</sub> alkenes (15–29 C%) and alkanes (7–33 C%). In the case of switchgrass and red oak, 70–74% of the carbon present in the samples was upgraded to hydrocarbons (the corresponding product distributions are provided in Table S3, ESI<sup>†</sup>). These results are significant as there have been very few attempts to upgrade the non-lignin water-soluble fraction but a recent techno-economic analysis (TEA) and life cycle assessment (LCA) study revealed that the entirety of the fractionation oil must be utilized to maximize product revenues and improve the cost efficiency of biorefineries.<sup>32</sup>

#### 2.4. Enzymatic hydrolysis of EtOH-insoluble pulp

We further performed the enzymatic hydrolysis on the EtOH insoluble pulp obtained from corn stover to investigate whether the cocktail enzymes could digest the sugars present upon





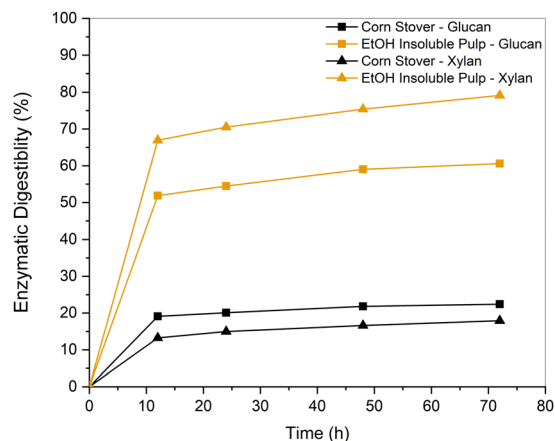


Fig. 13 Enzymatic digestion performed on EtOH-insoluble pulp and untreated corn stover as a control experiment at a digestion time of 72 h.

pretreatment. This analysis also helped rule out detrimental reactions between the reagents and sugars to which enzymes are sometimes sensitive. The results of the 72 h digestion are reported in Fig. 13 and Table S4 (ESI<sup>†</sup>). The residual solids showed a three-fold improvement in glucan and a four-fold improvement in xylan conversions compared to untreated biomass. Ferrini *et al.* stated that the quality of pulp obtained from RCF of biomass possessed superior quality compared to residual pulps obtained from organosolv fractionation. This was associated with the passivation of the lignin stream, which decreased the likelihood of lignin redeposition onto the fibers through recondensation processes.<sup>39</sup>

## 2.5. Remarks on the performance of the proposed approach for whole biomass upgrading in biorefineries

TEA/LCA studies highlighted the vital role of lignin valorization for biorefineries to become economically viable.<sup>19,32</sup> To this end, various strategies were explored to deconstruct lignocellulosic biomass into separate carbohydrate-rich and lignin-rich streams that could be individually upgraded to value-added products. “Lignin-first” strategies that release lignin from plant biomass were shown to be the most effective to provide a

processable lignin along with a cellulosic pulp amenable to bioethanol production.<sup>32,39,76</sup> Significant work focused on the release of lignin monomers and small oligomers that could find applications in inks, adhesives, and other high-value products.<sup>76–78</sup> However, there is a discrepancy between the size of these niche markets and the large volumes of bioethanol produced from the sugar-rich pulp. Therefore, pathways to commodity chemicals like mono-aromatics (benzene, toluene, xylene) and alkenes (ethylene, propylene, butene, butadiene) are significantly more attractive.<sup>19,77</sup> Recent TEA revealed that the coproduction of olefins and aromatics could lower the minimum selling price of ethanol from \$2 per gal to \$0.75 per gal.<sup>19</sup>

Several strategies were explored to convert “lignin-first” monomers to commodity aromatic hydrocarbons and oxygenates (phenol, cresol). However, very few studies tracked carbon atoms throughout the upgrading process, from the lignocellulosic feedstock to the final chemicals. The most comprehensive investigations to date are compiled in Table 1 and Table S5 (ESI<sup>†</sup>) and compared with the results obtained in the present work (our method for carbon tracking is provided in the ESI<sup>†</sup>). In their seminal *Science* article, the Sels group reported on the “lignin first” deconstruction and upgrading of birch and pine wood lignin to phenol, cresols, and propylene. They achieved a cumulative product yield of 33.3 wt% relative to the feedstock’s lignin fraction (12.8 wt% relative to whole biomass).<sup>76</sup> The Rinaldi group performed the hydrodeoxygenation of fractionated lignin-oil using a phosphidated Ni/SiO<sub>2</sub> catalyst. Aromatic and aliphatic hydrocarbons were produced with excellent yields under their reaction conditions, reaching 33.8 and 11.3 wt%, respectively, relative to lignin (10 wt% total relative to whole biomass).<sup>79</sup> However, these exceptional yields came at the expense of a broad product distribution ranging from C<sub>6</sub> to C<sub>20</sub>, with a large number of branched and di-aromatic compounds, which would preferentially find applications as biofuels.

In comparison, the present work produced 28.8 wt% of mono-aromatics, 4.0 wt% of C<sub>2</sub>–C<sub>6</sub> alkenes, and 8.7 wt% of C<sub>2</sub>–C<sub>6</sub> alkanes when processing red oak. Benzene, toluene, xylenes, ethylbenzene, and propylbenzene accounted for 79% and 85% of the mono-aromatics produced from the lignin and water-soluble fractions, respectively (Tables S2 and S3, ESI<sup>†</sup>).

Table 1 State-of-the-art results obtained for the lignin-first fractionation and upgrading of lignocellulosic biomass. The results obtained in the present work for red oak are provided for comparison. Additional comparisons are provided in Table S5 (ESI<sup>†</sup>)

Feedstock (reference)	Fractionation conditions	Upgrading conditions	Yield (wt% reference to lignin content)	Yield (wt% reference to mass of biomass)
Birchwood (Liao <i>et al.</i> ) <sup>76</sup>	235 °C, methanol, 5 wt% Ru/C, 30 bar H <sub>2</sub> , 3 h	Hydroprocessing 305 °C, 64 wt% Ni/SiO <sub>2</sub> Dealkylation	Phenol: 19.8 wt% Propylene: 9.3 wt% Cresols, benzenes, others: 4.2 wt%	Phenol: 7.1 wt% Propylene: 3.7 wt% Cresols, benzenes, others: 2.0 wt%
Poplar (Cao <i>et al.</i> ) <sup>79</sup>	180 °C, 2-propanol: water (7:3 v/v), RANEY <sup>®</sup> Ni, 3 h	410 °C, Z140-H HDO 300 °C, phosphidated Ni/SiO <sub>2</sub>	Aromatic C <sub>6</sub> –C <sub>10</sub> and C <sub>14</sub> –C <sub>20</sub> : 33.8 wt% Aliphatic C <sub>6</sub> –C <sub>10</sub> and C <sub>14</sub> –C <sub>20</sub> : 11.3 wt%	Aromatic C <sub>6</sub> –C <sub>10</sub> and C <sub>14</sub> –C <sub>20</sub> : 7.5 wt% Aliphatic C <sub>6</sub> –C <sub>10</sub> and C <sub>14</sub> –C <sub>20</sub> : 2.5 wt%
Red Oak (this work)	250 °C, ethanol, 5 wt% Pd/C, 30 bar H <sub>2</sub> , 3 h	Fast pyrolysis 500 °C HDO 400 °C, MoO <sub>3</sub>	Aromatics: 28.8 wt% Alkenes: 4.0 wt% Alkanes: 8.7 wt%	Aromatics: 9.5 wt% Alkenes: 3.3 wt% Alkanes: 5.2 wt%



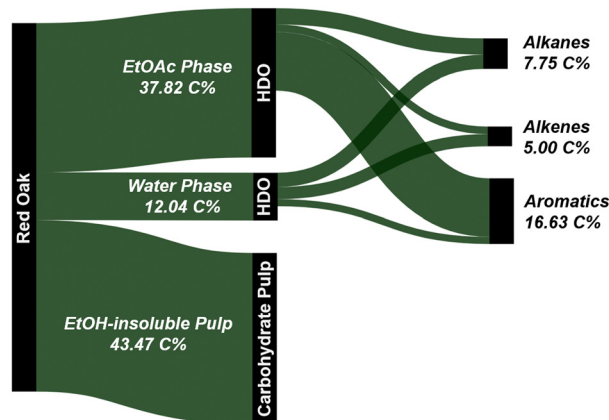


Fig. 14 Carbon flow (upper bound values) for the one-pot fractionation and pretreatment of whole biomass in EtOH at 250 °C using Pd/C followed by HDO of both the ethyl acetate and water fractions.

Similarly, ethylene, propylene, and butenes represented 45–47% of all the olefins produced from the two fractions. In addition to generating drop-in commodity chemicals, our approach achieved a cumulative hydrocarbon yield of 18.0 wt% relative to the initial biomass in the case of red oak, along with 98% glucan retention in the pulp (see Section 2.3 and Fig. 9). For completeness, we also tracked carbon atoms from raw red oak biomass to final products. As can be seen in Fig. 14, 29.4 C% of red oak was converted to hydrocarbons while 43.5 C% were recovered as highly amenable pulp, giving a total carbon recovery of 72.9%. Our approach also presents technical advantages as the hydrodeoxygenation was performed under ambient pressure conditions, overcoming the need for costly high-pressure reactors for this step.

Global warming potential (GWP) calculations are particularly challenging for emerging technologies due to the many parameters involved during technology optimization and scale up. Nevertheless, the TEA-LCA study by Bartling *et al.* for an ethanol biorefinery incorporating RCF is encouraging as it revealed that the valorization of the lignin fraction yields a GWP of  $-0.175$  kg CO<sub>2</sub> eq. per kg when ethanol is used as a solvent, hence a net decrease in CO<sub>2</sub> emissions.<sup>32</sup> Moreover, the calculated GWP did not consider the GWP of the petrochemicals that would be displaced by the corresponding bioproducts. The manufacture of fossil-derived platform alkenes and aromatics (ethylene, propylene, and benzene/toluene/xylene) is responsible for nearly 250 megatons of carbon dioxide equivalent per year.<sup>80</sup> Although a detailed TEA-LCA remains to be conducted for our approach, we anticipate that the advances presented here will further improve the GWP of lignin-first biorefineries and contribute to the decarbonization of the chemical industry.

### 3. Conclusion

The pretreatment of lignin was investigated using solvolytic and catalytic pretreatments to partially depolymerize it and enhance its conversion to aromatic hydrocarbons through CFP

and HDO reactions. EtOH was chosen as the reaction solvent due to its ability to solubilize and depolymerize lignin along with Pd/C, Ru/C, Pd/Al<sub>2</sub>O<sub>3</sub>, Ru/Al<sub>2</sub>O<sub>3</sub>, and Y zeolite catalysts at sub- and supercritical conditions. At 200 °C, nearly 60 wt% of the loaded corn stover organosolv lignin was isolated after 3 hours irrespective of the catalyst added. At supercritical conditions (250 °C), a reductive catalyst was required to suppress detrimental recondensation reactions. Elemental analysis showed that a greater extent of deoxygenation took place at 250 °C compared to 200 °C. It was also inferred that deoxygenation was carried out mainly through solvolytic deconstruction. In contrast, the transition metal catalysts are primarily involved in the hydrogenation of the products, as evidenced by the similar O/C ratios and varying H/C ratios.

The partially deconstructed samples' molecular weight distributions ranged between 1000 and 1386 Da using subcritical EtOH and 520–800 Da with supercritical EtOH. The volatile monomeric products obtained upon pretreatment of corn stover lignin as a function of various reaction conditions and catalysts were analyzed by GC-FID/MS. Higher monomeric product yields were obtained with supercritical EtOH than with subcritical EtOH (4.0–7.5 wt% *vs.* 1.5–4.0 wt%), and the product distribution greatly varied upon the catalyst used in the system.

The thermal characteristics of the pretreated samples and parent lignin samples were studied using TGA and proximate analysis. In general, a larger portion of the products was volatilized from the pretreated samples than from the parent lignin. These results were corroborated by the proximate analysis. Specifically, 83 wt% of the volatile fraction was observed for the sample pretreated using Pd/C catalyst in EtOH at 250 °C compared to 63 wt% for the parent lignin. During fast pyrolysis of the pretreated samples, the yield of pyrolytic char dropped from 58.4 C% for lignin down to 8.8 C% for the sample deconstructed at 250 °C using Pd/C, and it subsequently enhanced the formation of volatile species.

The lignin sample that was deconstructed using Pd/C and supercritical EtOH was subjected to upgrading to aromatic hydrocarbons through CFP and HDO routes, and the yields were significantly higher than that of the parent lignin (96% increase for CFP and 38% increase for HDO).

We extended this approach to the one-pot fractionation and pretreatment of lignin from whole biomass for low-carbon-footprint chemical production. The lignin oil generated through this pretreatment was funneled to platform hydrocarbons, while the carbohydrate pulp was amenable to bioethanol production. The yield of mono-aromatics, di-aromatics, and alkenes improved significantly upon one-pot pretreatment and fractionation of lignin from biomass using Pd/C catalyst at 250 °C (39–45 C%) compared to other technical lignin (16–26 C%) generated using conventional fractionation techniques. The same HDO conditions were subsequently applied to the carbohydrates-rich water-soluble fraction to reduce waste and improve the overall carbon efficiency of the studied process. This step generated primarily C<sub>2</sub>–C<sub>4</sub> alkenes and aromatic hydrocarbons. It also showed that all EtOH-soluble products could be upgraded using HDO, circumventing the need for a



costly extraction/separation step. Overall, the production of platform alkenes and aromatics increased by up to 174%, while the residual pulp was rich in sugars and 200% more digestible, making it more amenable to bioethanol production. The total carbon efficiency of the complete process, from raw biomass to final products, was 72.9%.

## 4. Experimental

### Chemicals and materials

Corn stover-derived organosolv lignin was obtained from Archer Daniels Midland (ADM). Renmatix lignin (RL) extracted from mixed hardwood using supercritical water extraction was provided by Renmatix and used without any further treatment. Indulin lignin (IL) extracted from pinewood is an unsulfonated kraft lignin obtained from Ingevity. Corn stover, switchgrass, and red oak biomass samples were provided by Iowa State University's BioCentury Research Farm. HPLC grade ethanol (EtOH, Decon Labs) was used as the reaction solvent for all experiments. Commercial 5 wt% Pd/C, 5 wt% Ru/C, 5 wt% Pd/Al<sub>2</sub>O<sub>3</sub>, 5 wt% Ru/Al<sub>2</sub>O<sub>3</sub> were purchased from Sigma-Aldrich and were used as received. HY zeolite (CBV 720 with SiO<sub>2</sub>/Al<sub>2</sub>O<sub>3</sub> = 30) and ZSM-5 (CBV 3024E with SiO<sub>2</sub>/Al<sub>2</sub>O<sub>3</sub> = 30 in its ammonium form) were purchased from Zeolyst International. The purchased NH<sub>4</sub>-ZSM-5 was calcined in air at 550 °C for 10 hours (ramp: 5 °C min<sup>-1</sup>) to obtain the acidic form HZSM-5 of the zeolite before catalytic testing. MoO<sub>3</sub> (Sigma-Aldrich, reagent grade) was calcined in a muffle furnace at 550 °C prior to catalytic testing. Polystyrene standards purchased from Agilent (Agilent Technologies, Inc., Santa Clara, CA) were used to calibrate molecular weights as a function of retention times for the GPC analysis. Tetrahydrofuran (Certified), which contains about 0.025% butylated hydroxytoluene as a preservative, was purchased from Fisher Scientific. For a complete list of commercial standards used for gas chromatography calibration, the reader is kindly referred to the ESI<sup>†</sup> (Table S6).

### Lignin pretreatment

Approximately 200 mg of lignin was added to 40 mL EtOH in a 75 mL Parr 4590 reactor along with 40 mg of the catalyst. After the reactor was sealed, it was purged three times with nitrogen. Next, the reactor was charged with 30 bar of hydrogen at room temperature. The reactor was then heated to either 200 or 250 °C (ramp: 10 °C min<sup>-1</sup>) and held at the target temperature for 3 h while stirring at 400 rpm. The pressure in the reaction vessel reached 70 bar at 200 °C and 110 bar at 250 °C. After the reaction, the reactor was cooled and depressurized at room temperature.

Approximately 1.5 mL of the product dissolved in the solvent was collected, filtered using a 0.22 µm nylon syringe filter, and subjected to GC-FID/MS analysis. The remaining reactor content was recovered, the reactor was washed thoroughly with excess solvent, and the two solutions were combined in the same beaker. The mixture was then filtered using a 0.2 µm poly(ether sulfone) filter to separate the catalyst, and the obtained filtrate was dried. It is important to note that char

and very high molecular weight oligomers are insoluble in EtOH at room temperature and were thus not recovered after pretreatment. The mass of the sample obtained after pretreatment was measured after drying it in a vacuum oven overnight at 40 °C. The obtained pretreated samples were further characterized through GPC, elemental analysis, HSQC NMR, and TGA analysis.

### Fast pyrolysis of the parent lignin and pretreated samples

Untreated lignin and the pretreated samples were pyrolyzed in a two-stage Frontier tandem micro-pyrolyzer system (Frontier laboratory, Japan) equipped with an auto-shot sampler (Rx-3050 TR, Frontier Laboratories, Japan) connected to an Agilent 7890B GC-FID/TCD/MS (Fig. S10, ESI<sup>†</sup>). A deactivated stainless-steel cup containing approximately 500 µg of the sample was dropped into a first-stage reactor preheated at 500 °C, where the sample was pyrolyzed. Prior investigations have shown that the heating rate for this system is 500 °C s<sup>-1</sup>.<sup>81</sup> Helium gas was used as both the sweep and carrier gas (Fig. S11, ESI<sup>†</sup>). The second-stage reactor was maintained at 300 °C to avoid condensation of the pyrolytic products. The vapors exiting the pyrolyzer were directly carried to the online GC for analysis. Char yields were measured gravimetrically by weighing the sample cups before and after pyrolysis. For the purpose of reporting on carbon yields, the carbon content of char was assumed to be approximately 90% based on previous reports.<sup>82</sup>

### CFP and HDO

CFP and HDO reactions were carried out in the same micro-pyrolyzer system as the one used for fast pyrolysis. For CFP, a quartz tube containing approximately 10 mg of the zeolite catalyst (210–297 µm) was inserted in the second-stage reactor to act as a packed bed reactor (Fig. S12, ESI<sup>†</sup>). The pyrolysis reactor and the catalyst bed temperatures were both set at 500 °C.

For HDO, hydrogen gas was used as the sweep and carrier gas. The pyrolyzer and the second stage reactor were kept at 500 and 400 °C, respectively. Approximately 10 mg of MoO<sub>3</sub> (37–105 µm) catalyst was mixed with ~70 mg acid-washed glass beads (149–210 µm), fixed between two layers of quartz wool, and placed in the second reactor. The catalyst was reduced at 400 °C for 1 h *in situ* before reaction. The product yields were determined based on the following formula:

Yield of products (C%) =

$$\frac{\text{Mass of product(mg)} \times \text{carbon content in product}}{\text{Mass of sample(mg)} \times \text{carbon content of sample}} \times 100$$

All interfaces, including the GC inlet, were kept at 300 °C to minimize condensation and repolymerization of generated vapors. The glass beads and quartz wool were previously tested and found to be inactive under reaction conditions.<sup>19</sup>





## One-pot fractionation and pretreatment of lignin from biomass

Approximately 1 g of biomass with a particle size  $\leq 2$  mm, 100 mg of 5 wt% Pd/C, and 40 mL EtOH were added to a 75 mL Parr 4590 reactor. The reactor was sealed and purged with nitrogen three times. Next, the reactor was pressurized with 30 bar of hydrogen, heated to 250 °C (at a heating rate of 10 °C min<sup>-1</sup>), and held for 3 h while stirring at 400 rpm. To obtain an adequate amount of sample for further characterization, all experiments were repeated for a minimum of 5 times.

After the reaction, the reactor was cooled down to room temperature and depressurized. The solid residue (Pd/C and EtOH-insoluble pulp) was separated by filtering the reactor contents using a 0.2  $\mu$ m poly(ether sulfone) filter and washed with 30 mL EtOH. The catalyst was separated from the EtOH-insoluble pulp using a 75  $\mu$ m sieve. EtOH was evaporated from the EtOH-soluble products by drying the filtrate overnight in a vacuum oven. The starting biomass, the EtOH-insoluble pulp, and the EtOH-soluble products were subjected to composition analysis to perform an overall mass and component balance. The EtOH-insoluble pulp obtained from corn stover was also subjected to enzymatic hydrolysis to determine the digestibility of pulp compared to the parent corn stover.

To separate the soluble lignin- and carbohydrates-derived products present in the EtOH-soluble fraction, liquid-liquid extractions were performed three times with ethyl acetate and water. The lignin oil was mainly concentrated in the ethyl acetate phase, while the aqueous phase contained dissolved sugars.<sup>69,83</sup> The pretreated lignin oil was recovered by evaporating the ethyl acetate from the sample in a vacuum oven at 40 °C. The obtained lignin oil was characterized by GC-FID/MS, GPC, elemental analysis and further upgraded using CFP and HDO. Similarly, the sugar rich aqueous fraction was evaporated to remove water using a vacuum oven at 40 °C for two days. The dried sugar fraction obtained was also subjected to catalytic upgrading through HDO.

## Author contributions

The manuscript was written through contributions of all authors. All authors have given approval to the final version of the manuscript.

## Conflicts of interest

There are no conflicts to declare.

## Acknowledgements

This material is based upon work supported by the National Science Foundation under the grant number CBET-1706046 and JPT's Richard C. Seagrave Professorship. The authors thank Iowa State University's BioCentury research farm for the biomass samples. We also acknowledge Dr Patrick Johnston for help with GPC and other analyses.

## References

- 1 V. Menon and M. Rao, *Prog. Energy Combust. Sci.*, 2012, **38**, 522–550.
- 2 Z. Sun, B. Fridrich, A. de Santi, S. Elangovan and K. Barta, *Chem. Rev.*, 2018, **118**, 614–678.
- 3 M. Lievonen, J. J. Valle-Delgado, M.-L. Mattinen, E.-L. Hult, K. Lintinen, M. A. Kostianen, A. Paananen, G. R. Szilvay, H. Setälä and M. Österberg, *Green Chem.*, 2016, **18**, 1416–1422.
- 4 C. C. Xu, L. Dessbesell, Y. Zhang and Z. Yuan, *Biofuels, Bioprod. Biorefin.*, 2020, **15**, 32–36.
- 5 A. Saraeian, M. W. Nolte and B. H. Shanks, *Renewable Sustainable Energy Rev.*, 2019, **104**, 262–280.
- 6 A. V. Bridgwater, *Biomass Bioenergy*, 2012, **38**, 68–94.
- 7 G. W. Huber, S. Iborra and A. Corma, *Chem. Rev.*, 2006, **106**, 4044–4098.
- 8 A. Oasmaa, D. C. Elliott and J. Korhonen, *Energy Fuels*, 2010, **24**, 6548–6554.
- 9 A. Eschenbacher, P. Fennell and A. D. Jensen, *Energy Fuels*, 2021, **35**, 18333–18369.
- 10 L. Fan, Y. Zhang, S. Liu, N. Zhou, P. Chen, Y. Cheng, M. Addy, Q. Lu, M. M. Omar, Y. Liu, Y. Wang, L. Dai, E. Anderson, P. Peng, H. Lei and R. Ruan, *Bioresour. Technol.*, 2017, **241**, 1118–1126.
- 11 T. R. Carlson, Y.-T. Cheng, J. Jae and G. W. Huber, *Energy Environ. Sci.*, 2011, **4**, 145–161.
- 12 D. J. Mihalcik, C. A. Mullen and A. A. Boateng, *J. Anal. Appl. Pyrolysis*, 2011, **92**, 224–232.
- 13 Y. Yu, X. Li, L. Su, Y. Zhang, Y. Wang and H. Zhang, *Appl. Catal., A*, 2012, **447–448**, 115–123.
- 14 S. Kelkar, C. M. Saffron, K. Andreassi, Z. Li, A. Murkute, D. J. Miller, T. J. Pinnavaia and R. M. Krieger, *Appl. Catal., B*, 2015, **174**, 85–95.
- 15 T. Prasomsri, T. Nimmanwudipong and Y. Román-Leshkov, *Energy Environ. Sci.*, 2013, **6**, 1732–1738.
- 16 M. W. Nolte, J. Zhang and B. H. Shanks, *Green Chem.*, 2016, **18**, 134–138.
- 17 G. Zhou, P. A. Jensen, D. M. Le, N. O. Knudsen and A. D. Jensen, *Green Chem.*, 2016, **18**, 1965–1975.
- 18 H. Zhang, T. R. Carlson, R. Xiao and G. W. Huber, *Green Chem.*, 2012, **14**, 98–110.
- 19 A. Saraeian, A. Aui, Y. Gao, M. M. Wright, M. Foston and B. H. Shanks, *Green Chem.*, 2020, **22**, 2513–2525.
- 20 M. W. Nolte, A. Saraeian and B. H. Shanks, *Green Chem.*, 2017, **19**, 3654–3664.
- 21 K. B. Ansari, J. S. Arora, J. W. Chew, P. J. Dauenhauer and S. H. Mushrif, *Ind. Eng. Chem. Res.*, 2019, **58**, 15838–15852.
- 22 M. Carrier, M. Windt, B. Ziegler, J. Appelt, B. Saake, D. Meier and A. Bridgwater, *ChemSusChem*, 2017, **10**, 3212–3224.
- 23 P. D. Muley, C. Henkel, K. K. Abdollahi, C. Marculescu and D. Boldor, *Energy Convers. Manage.*, 2016, **117**, 273–280.
- 24 A. R. Stanton, K. Iisa, C. Mukarakate and M. R. Nimlos, *ACS Sustainable Chem. Eng.*, 2018, **6**, 10030–10038.
- 25 Y. Feng, G. Li, X. Li, N. Zhu, B. Xiao, J. Li and Y. Wang, *Bioresour. Technol.*, 2016, **214**, 520–527.



- 26 Z. Ma, A. Ghosh, N. Asthana and J. van Bokhoven, *ChemCatChem*, 2017, **9**, 954–961.
- 27 J. Akhtar and N. A. S. Amin, *Renewable Sustainable Energy Rev.*, 2011, **15**, 1615–1624.
- 28 H.-j Huang and X.-z Yuan, *Prog. Energy Combust. Sci.*, 2015, **49**, 59–80.
- 29 M. Y. Lui, B. Chan, A. K. L. Yuen, A. F. Masters, A. Montoya and T. Maschmeyer, *ChemSusChem*, 2017, **10**, 2140–2144.
- 30 S. Van den Bosch, W. Schutyser, R. Vanholme, T. Driessen, S. F. Koelewijn, T. Renders, B. De Meester, W. J. J. Huijgen, W. Dehaen, C. M. Courtin, B. Lagrain, W. Boerjan and B. F. Sels, *Energy Environ. Sci.*, 2015, **8**, 1748–1763.
- 31 W. Schutyser, S. Van den Bosch, T. Renders, T. De Boe, S. F. Koelewijn, A. Dewaele, T. Ennaert, O. Verkinderen, B. Goderis, C. M. Courtin and B. F. Sels, *Green Chem.*, 2015, **17**, 5035–5045.
- 32 A. W. Bartling, M. L. Stone, R. J. Hanes, A. Bhatt, Y. Zhang, M. J. Bidy, R. Davis, J. S. Kruger, N. E. Thornburg, J. S. Luterbacher, R. Rinaldi, J. S. M. Samec, B. F. Sels, Y. Román-Leshkov and G. T. Beckham, *Energy Environ. Sci.*, 2021, **14**, 4147–4168.
- 33 D. Vincent Sahayaraj, L. A, E. M. Mitchell, X. Bai and J.-P. Tessonnier, *Green Chem.*, 2021, **23**, 7731–7742.
- 34 E. M. Anderson, R. Katahira, M. Reed, M. G. Resch, E. M. Karp, G. T. Beckham and Y. Román-Leshkov, *ACS Sustainable Chem. Eng.*, 2016, **4**, 6940–6950.
- 35 J.-Y. Kim, S. Oh, H. Hwang, T.-S. Cho, I.-G. Choi and J. W. Choi, *Chemosphere*, 2013, **93**, 1755–1764.
- 36 R. J. A. Gosselink, W. Teunissen, J. E. G. van Dam, E. de Jong, G. Gellerstedt, E. L. Scott and J. P. M. Sanders, *Bioresour. Technol.*, 2012, **106**, 173–177.
- 37 S. Van den Bosch, T. Renders, S. Kennis, S. F. Koelewijn, G. Van den Bossche, T. Vangeel, A. Deneyer, D. Depuydt, C. M. Courtin, J. M. Thevelein, W. Schutyser and B. F. Sels, *Green Chem.*, 2017, **19**, 3313–3326.
- 38 O. E. Ebikade, N. Samulewicz, S. Xuan, J. D. Sheehan, C. Wu and D. G. Vlachos, *Green Chem.*, 2020, **22**, 7435–7447.
- 39 P. Ferrini, C. A. Rezende and R. Rinaldi, *ChemSusChem*, 2016, **9**, 3171–3180.
- 40 S. Ghoreishi, T. Barth and D. H. Hermundsgard, *ACS Omega*, 2019, **4**, 19265–19278.
- 41 L. Chen, A. P. van Muyden, X. Cui, Z. Fei, N. Yan, G. Laurenczy and P. J. Dyson, *JACS Au*, 2021, **1**, 729–733.
- 42 S. Van den Bosch, T. Renders, S. Kennis, S. F. Koelewijn, G. Van den Bossche, T. Vangeel, A. Deneyer, D. Depuydt, C. M. Courtin, J. M. Thevelein, W. Schutyser and B. F. Sels, *Green Chem.*, 2017, **19**, 3313–3326.
- 43 S. Qiu, M. Wang, Y. Fang and T. Tan, *Sustainable Energy Fuels*, 2020, **4**, 5588–5594.
- 44 T. Vangeel, T. Renders, K. Van Aelst, E. Cooreman, S. Van den Bosch, G. Van den Bossche, S. F. Koelewijn, C. M. Courtin and B. F. Sels, *Green Chem.*, 2019, **21**, 5841–5851.
- 45 J. Park, H. S. Cahyadi, U. Mushtaq, D. Verma, D. Han, K.-W. Nam, S. K. Kwak and J. Kim, *ACS Catal.*, 2020, **10**, 12487–12506.
- 46 A. Bjelić, M. Grilc, M. Huš and B. Likozar, *Chem. Eng. J.*, 2019, **359**, 305–320.
- 47 R. Shu, Q. Zhang, L. Ma, Y. Xu, P. Chen, C. Wang and T. Wang, *Bioresour. Technol.*, 2016, **221**, 568–575.
- 48 F. Lu and J. Ralph, *J. Agric. Food Chem.*, 1999, **47**, 1988–1992.
- 49 H. Luo, I. M. Klein, Y. Jiang, H. Zhu, B. Liu, H. I. Kenttämä and M. M. Abu-Omar, *ACS Sustainable Chem. Eng.*, 2016, **4**, 2316–2322.
- 50 Y. Ye, Y. Zhang, J. Fan and J. Chang, *Bioresour. Technol.*, 2012, **118**, 648–651.
- 51 Y. Ye, Y. Zhang, J. Fan and J. Chang, *Ind. Eng. Chem. Res.*, 2011, **51**, 103–110.
- 52 S. Van den Bosch, W. Schutyser, S. F. Koelewijn, T. Renders, C. M. Courtin and B. F. Sels, *Chem. Commun.*, 2015, **51**, 13158–13161.
- 53 R. M. Kalinoski, W. Li, J. K. Mobley, S. O. Asare, M. Dorrani, B. C. Lynn, X. Chen and J. Shi, *ACS Sustainable Chem. Eng.*, 2020, **8**, 18455–18467.
- 54 P. Halder, S. Kundu, S. Patel, R. Parthasarathy, B. Pramanik, J. Paz-Ferreiro and K. Shah, *Energy Convers. Manage.*, 2019, **200**, 112067.
- 55 N. Muhammad, Z. Man, M. A. Bustam, M. I. A. Mutalib and S. Rafiq, *J. Ind. Eng. Chem.*, 2013, **19**, 207–214.
- 56 M. Wądrzyk, R. Janus, M. Lewandowski and A. Magdziarz, *Renewable Energy*, 2021, **177**, 942–952.
- 57 S. Wang, K. Wang, Q. Liu, Y. Gu, Z. Luo, K. Cen and T. Fransson, *Biotechnol. Adv.*, 2009, **27**, 562–567.
- 58 S. Zhou, Y. Xue, A. Sharma and X. Bai, *ACS Sustainable Chem. Eng.*, 2016, **4**, 6608–6617.
- 59 D. Duan, H. Lei, Y. Wang, R. Ruan, Y. Liu, L. Ding, Y. Zhang and L. Liu, *J. Cleaner Prod.*, 2019, **231**, 331–340.
- 60 Z.-P. Lei, Z.-Q. Hu, H.-F. Shui, S.-B. Ren, Z.-C. Wang, S.-G. Kang and C.-X. Pan, *Fuel Process. Technol.*, 2015, **138**, 612–615.
- 61 T. Hosoya, H. Kawamoto and S. Saka, *J. Anal. Appl. Pyrolysis*, 2009, **85**, 237–246.
- 62 X. Bai, K. H. Kim, R. C. Brown, E. Dalluge, C. Hutchinson, Y. J. Lee and D. Dalluge, *Fuel*, 2014, **128**, 170–179.
- 63 T. Hosoya, H. Kawamoto and S. Saka, *J. Anal. Appl. Pyrolysis*, 2009, **84**, 79–83.
- 64 Y.-C. Qu, Z. Wang, Q. Lu and Y. Zhang, *Ind. Eng. Chem. Res.*, 2013, **52**, 12771–12776.
- 65 C. Liu, X. Wang, F. Lin, H. Zhang and R. Xiao, *Fuel Process. Technol.*, 2018, **169**, 50–57.
- 66 P. S. Marathe, R. J. M. Westerhof and S. R. A. Kersten, *Appl. Energy*, 2019, **236**, 1125–1137.
- 67 K. Wang, K. H. Kim and R. C. Brown, *Green Chem.*, 2014, **16**, 727–735.
- 68 A. Saraeian, S. J. Burkhov, D. Jing, E. A. Smith and B. H. Shanks, *ACS Sustainable Chem. Eng.*, 2021, **9**, 6685–6696.
- 69 W. Guan, X. Chen, C. W. Tsang, H. Hu and C. Liang, *ACS Sustainable Chem. Eng.*, 2021, **9**, 3529–3541.
- 70 M. M. Abu-Omar, K. Barta, G. T. Beckham, J. S. Luterbacher, J. Ralph, R. Rinaldi, Y. Román-Leshkov, J. S. M. Samec, B. F. Sels and F. Wang, *Energy Environ. Sci.*, 2021, **14**, 262–292.



- 71 Z. Zhang, M. D. Harrison, D. W. Rackemann, W. O. S. Doherty and I. M. O'Hara, *Green Chem.*, 2016, **18**, 360–381.
- 72 P. Sannigrahi, A. J. Ragauskas and S. J. Miller, *Energy Fuels*, 2010, **24**, 683–689.
- 73 T. Phongpreecha, N. C. Hool, R. J. Stoklosa, A. S. Klett, C. E. Foster, A. Bhalla, D. Holmes, M. C. Thies and D. B. Hodge, *Green Chem.*, 2017, **19**, 5131–5143.
- 74 Z. Luo, K. Lu, Y. Yang, S. Li and G. Li, *RSC Adv.*, 2019, **9**, 31960–31968.
- 75 G. Zhou, P. A. Jensen, D. M. Le, N. O. Knudsen and A. D. Jensen, *ACS Sustainable Chem. Eng.*, 2016, **4**, 5432–5440.
- 76 Y. Liao, S.-F. Koelewijn, G. V. D. Bossche, J. V. Aelst, S. V. D. Bosch, T. Renders, K. Navare, T. Nicolai, K. V. Aelst, M. Maesen, H. Matsushima, J. M. Thevelein, K. V. Acker, B. Lagrain, D. Verboekend and B. F. Sels, *Science*, 2020, **367**, 1385–1390.
- 77 Z. Sun, J. Cheng, D. Wang, T.-Q. Yuan, G. Song and K. Barta, *ChemSusChem*, 2020, **13**, 5199–5212.
- 78 Z. Sun, G. Bottari, A. Afanassenko, M. C. A. Stuart, P. J. Deuss, B. Fridrich and K. Barta, *Nat. Catal.*, 2018, **1**, 82–92.
- 79 Z. Cao, M. Dierks, M. T. Clough, I. B. Daltro de Castro and R. Rinaldi, *Joule*, 2018, **2**, 1118–1133.
- 80 IEA, *Technology Roadmap - Energy and GHG Reductions in the Chemical Industry via Catalytic Processes*, IEA, Paris, 2013, <https://www.iea.org/reports/technology-roadmap-energy-and-ghg-reductions-in-the-chemical-industry-via-catalytic-processes>.
- 81 J. Zhang, M. W. Nolte and B. H. Shanks, *ACS Sustainable Chem. Eng.*, 2014, **2**, 2820–2830.
- 82 R. K. Sharma, J. B. Wooten, V. L. Baliga, X. Lin, W. Geoffrey Chan and M. R. Hajaligol, *Fuel*, 2004, **83**, 1469–1482.
- 83 T. Guo, X. Li, X. Liu, Y. Guo and Y. Wang, *ChemSusChem*, 2018, **11**, 2758–2765.

